Journal of proteome research

Article

Cite This: J. Proteome Res. 2020, 19, 279−291

pubs.acs.org/jpr

Characterization of the Proteomic Response of A549 Cells Following Sequential Exposure to *Aspergillus fumigatus* and *Pseudomonas aeruginosa*

Anatte Margalit, Kevin Kavanagh,* and James C. Carolan

Department of Biology, Maynooth University, Maynooth, Co. Kildare W23F2H6, Ireland

Supporting Information

ABSTRACT: *Aspergillus fumigatus* and *Pseudomonas aeruginosa* are the most prevalent fungal and bacterial pathogens associated with cystic-fibrosis-related infections, respectively. *P. aeruginosa* eventually predominates as the primary pathogen, though it is unknown why this is the case. Label-free quantitative proteomics was employed to investigate the cellular response of the alveolar epithelial cell line, A549, to coexposure of *A. fumigatus* and *P. aeruginosa*. These studies revealed a significant increase in the rate of *P. aeruginosa* proliferation where *A. fumigatus* was present. Shotgun proteomics performed on A549 cells exposed to either *A. fumigatus* or *P. aeruginosa* or to *A. fumigatus* and *P. aeruginosa* sequentially revealed distinct changes to the host cell proteome in response to either or both pathogens. While key signatures of infection were retained among all pathogen-exposed groups, including changes in mitochondrial activity and energy output, the relative abundance of proteins associated with endocytosis, phagosomes, and lysosomes was decreased in sequentially exposed cells compared to cells exposed to either pathogen. Our findings indicate that *A. fumigatus* renders A549 cells unable to internalize bacteria, thus providing an environment in which *P. aeruginosa* can proliferate. This research provides novel insights into the whole-cell proteomic response of A549 cells to *A. fumigatus* and *P. aeruginosa* and highlights distinct differences in the proteome following sequential exposure to both pathogens, which may explain why *P. aeruginosa* can predominate.

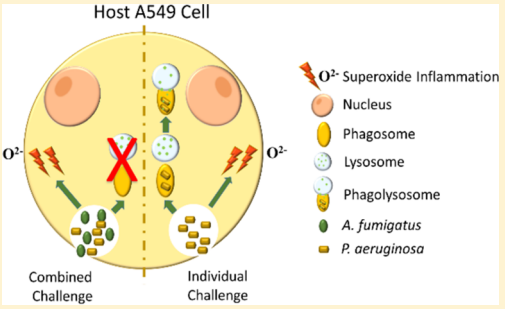

KEYWORDS: *Aspergillus, cellular response, cystic fibrosis, fungal infection, Pseudomonas*

INTRODUCTION

The lungs of cystic fibrosis (CF) patients are colonized by a variety of bacterial and fungal pathogens, which affect pulmonary function and contribute to mortality. These include the fungus *Aspergillus fumigatus* (A.f.) and the bacterium *Pseudomonas aeruginosa* (P.a.), which are frequently present in the CF airways. The pulmonary epithelium is the first point of contact for these pathogens and their host.[1,2] Determining how host cells respond to these pathogens and how these microorganisms interact with each other is key to understanding how pulmonary infection develops in the lung.[3−7] *P. aeruginosa* is recognized as the primary cause of morbidity and mortality within the CF community, and it is estimated that 80% of CF sufferers are chronically infected with *P. aeruginosa* by the age of 20.[7−9] Its ability to survive in the CF environment gives *P. aeruginosa* a distinct advantage over other microbial species within the lung, and once established, chronic infection by these pathogens is rarely eradicated.[6,10,11] To survive in the CF lung, *P. aeruginosa* must overcome several challenges from the host immune response including oxidative stress, osmotic stress due to an abnormal airway surface liquid, limited nutrients, and exposure to antibiotics. A consequence of long-term exposure to antibiotics is the emergence of antibiotic-resistant strains of *P. aeruginosa*.[12] These factors and an arsenal of secreted virulent exoproducts such as pyocyanin (PCN), rhamnolipids, hemolysin, proteases, and elastase enable *P. aeruginosa* to mediate pathogenesis in the CF airways.[13,14]

The most prevalent fungal pathogen associated with the CF lung is *A. fumigatus*, which is detected in up to 57% of CF patients.[14,15] *A. fumigatus* is ubiquitous in the environment where it forms and releases airborne conidia, which measure 2−3 μm in diameter and is thus easily transported through the respiratory tract when inhaled. For immunocompetent individuals, this is of little consequence and incoming conidia are quickly eliminated by the pulmonary immune system.[16−18] In the immunocompromised airways, as observed in CF, conidia that avoid elimination can germinate and provoke a proinflammatory immune response triggered by the secretion of toxins and allergens from the developing fungus. This can result in the manifestation of a hypersensitivity disorder, allergic bronchopulmonary aspergillosis (ABPA), which affects up to 13% of asthmatics and CF patients.[19−21] Several factors contribute to persistent *A. fumigatus* infection within the CF lung including its ability to adapt to the challenging

Received: August 2, 2019
Published: November 6, 2019

DOI: 10.1021/acs.jproteome.9b00520
J. Proteome Res. 2020, 19, 279−291

environment of the CF lung, such as hypoxia, oxidative stress, and nutrient limitations, thus enabling *A. fumigatus* to establish chronic or recurring infections in the respiratory tract.[22] The production of *A. fumigatus* secondary metabolites such as gliotoxin and fumagillin retards the mucociliary elevator and inhibits macrophage and neutrophil activity, thereby impairing the primary immune response.[18,23] *A. fumigatus* is reported to be the only species associated with an increased risk of *P. aeruginosa* colonization in CF, and coinfection by *A. fumigatus* and *P. aeruginosa* is more detrimental to the host than infection by either pathogen.[5,24−26] This may be due, in part, to an increase in the secretion of toxic compounds resulting from pathogen−host and intermicrobial interactions.[27]

Although *A. fumigatus* or *P. aeruginosa* can represent a major threat to the CF sufferer, very little is known about how the host cell responds at the molecular level to infection by these pathogens when present in combination. To address this knowledge gap, label-free quantitative (LFQ) proteomics was employed to investigate the response of A549 cells to sequential infection by *A. fumigatus* and *P. aeruginosa*. The A549 cell line is a well-established in vitro model system for studying pathogen−host interactions on the alveolar cell surface of the lung, particularly in the context of *A. fumigatus* and *P. aeruginosa* infections.[28−34] Research to date has focused on the response of A549 cells to either *A. fumigatus* or *P. aeruginosa* exposure; however, a better understanding of the cellular response to coinfection is required to inform future therapeutic strategies. Our preliminary experiments revealed that the replication of *P. aeruginosa* increased exponentially in the presence of *A. fumigatus*, allowing us to generate a hypothesis that *A. fumigatus* promotes the growth of *P. aeruginosa*, which was subsequently validated. To investigate this further, and to specifically determine how a sequential infection differs from an individual one, we then conducted comparative LFQ analysis on A549 cells exposed to *A. fumigatus* or *P. aeruginosa* or sequential exposure to both pathogens. The proteomic data presented here provides an explanation as to why, in the context of coinfection, *P. aeruginosa* predominates over *A. fumigatus* and reveals an important role for A549 cells in facilitating bacterial survival and proliferation. This whole-system analysis approach provides novel insights into the cellular response to polymicrobial challenges and the potential strategies employed by pathogens to modulate and manipulate their hosts.

EXPERIMENTAL SECTION

Cell Culture

A549 cells (ATCC CCL 185, derived from a human lung carcinoma) were cultured in a 25 cm^2 tissue culture flask (Sarstedt) containing "cell culture medium" [Dulbecco's modified Eagle's medium (DMEM) (95% v/v) (Sigma-Aldrich)] supplemented with 5% (v/v) fetal calf serum (FCS, Gibco) and 2% L-glutamine (Gibco) and incubated at 37 °C and 5% CO_2 in a humidified atmosphere. Cells were subcultured by trypsinization every 3−4 days.

Preparation of *A. fumigatus*

A. fumigatus (ATCC 26933) was grown on Sabouraud dextrose agar (Oxoid). Conidia were harvested using 0.01% Tween-80 and washed twice in phosphate-buffered saline (PBS). Conidial number was determined by hemocytometry, and conidia were resuspended in a cell culture medium.

Preparation of *P. aeruginosa*

P. aeruginosa (PAO1) was cultured in a nutrient broth (Oxoid) for 24 h at 37 °C in an orbital incubator. The concentration of the bacteria in the suspension was measured by obtaining the optical density at 600 nm (OD_{600}), where OD1 represented approximately 3×10^8 colony-forming units (CFU)/mL. Bacteria were washed twice with PBS and resuspended in a cell culture medium.

Exposure of A549 Cells to *A. fumigatus* and *P. aeruginosa* or Coexposure

T25 flasks were seeded with A549 cells (5×10^5 cells per T25 flask) and incubated for 24 h. On the day of exposure, the culture medium was removed and fresh culture medium was added. Aliquots of the conidial (2×10^4 conidia/mL) or bacterial suspension (1×10^6 CFU/mL) were added to each subconfluent flask of A549 cells (8×10^5 cells per T25 flask) ($n = 3$). To coexpose the A549 cells, a final concentration of 2×10^4 conidia/mL and 2×10^5 CFU/mL was added to each flask ($n = 3$). The lower inoculum of the bacteria was to account for the prior exposure to conidia. Controls were unexposed ($n = 3$). A549 cells were incubated for 12 h as described previously, before being subjected to protein extraction.

Sequential Exposure of A549 Cells to *A. fumigatus* and *P. aeruginosa*

A549 cells were incubated with *A. fumigatus* (2×10^4 conidia/mL) for 8 h, after which *P. aeruginosa* (2×10^5 CFU/mL) was added to each of the flasks and incubated for a further 4 h to give a total incubation period of 12 h ($n = 3$). Separately, *A. fumigatus* and *P. aeruginosa* were cultured at these densities, for 8 and 4 h, respectively ($n = 3$). Unexposed A549 cells were incubated for 12 h ($n = 3$). Proteins were extracted from the A549 cells after each time point.

Bacterial Proliferation Assays

Aliquots of media were removed from flasks of A549 cells coexposed to *A. fumigatus* (2×10^4 conidia/mL) and *P. aeruginosa* (2×10^5 CFU/mL) or with *P. aeruginosa* alone (1×10^6 CFU/mL) at 0 and 12 h, and diluted several times in PBS ($n = 4$). Bacterial dilutions were spread on nutrient agar plates containing amphotericin B (12.5 μg/50 μL, Gibco) and incubated for 24 h at 37 °C. CFU counts were performed, and growth was measured as a percentage of the CFU count taken from the flasks prior to incubation (0 h).

P. aeruginosa Cultured in the Absence of A549 Cells

P. aeruginosa was incubated at a density of 1×10^6 CFU/mL with and without *A. fumigatus* (2×10^4 conidia/mL) in a cell culture medium for 12 h and at a density of 2×10^5/mL for 4 h ($n = 4$). CFU counts were performed on the higher density at 0 and 12 h and on the lower density at 0, 2, and 4 h ($n = 4$).

P. aeruginosa Cultured in Coculture Supernatant

P. aeruginosa (1×10^6 CFU/mL) was incubated with ($n = 4$) and without *A. fumigatus* (2×10^4 conidia/mL) in a cell culture medium for 12 h in the absence of A549 cells ($n = 4$). The supernatants from the individual culture and coculture were filter-sterilized through 0.2 μm filters (Filtropur S 0.2 Sarstedt) and added to sterile flasks. *P. aeruginosa* was added to give a final concentration of 1×10^6 CFU/mL. The bacterial suspension was incubated for 12 h, and CFU counts were performed as described previously.

DOI: 10.1021/acs.jproteome.9b00520
J. Proteome Res. 2020, 19, 279−291

Sample Preparation for Label-Free Quantitative Mass Spectrometry (LFQ/MS)

A549 cells were harvested by trypsinization using a 1 mL trypsin buffer [trypsin (0.25% w/v)−ethylenediaminetetraacetic acid (0.022% w/v) in PBS] for 5 min or until the cells had detached. An equal volume of trypsin neutralization medium (DMEM 95% v/v) FCS (5% v/v) was added to inhibit the action of trypsin, followed by centrifugation of the cell suspension at 200*g* for 5 min. The cell pellet was resuspended in 3 mL PBS, and the centrifugation step was repeated. Ex situ cell lysis was performed by resuspending the cell pellet in a 500 μL cell lysis buffer [8 M urea, 2 M thiourea, and 0.1 M Tris−HCl (pH 8.0) dissolved in high-performance liquid chromatography (HPLC)-grade dH_2O], supplemented with protease inhibitors [aprotinin, leupeptin, pepstatin A, and tosyl-L-lysyl-chloromethane hydrochloride (10 μg/mL), Sigma-Aldrich] and phosphatase inhibitors (phosphatase inhibitor cocktail 2, Sigma-Aldrich). Cell lysates were kept at room temperature on a rotary wheel (Stuart Rotator SB2, Bibby Scientific Limited, Staffordshire, U.K.) for 2 h. The cell lysate was subjected to centrifugation (Eppendorf Centrifuge 5418) for 5 min at 14 500*g* to pellet cellular debris. The supernatant was removed and quantified using the Bradford method. Each sample (100 μg) was subjected to overnight acetone precipitation. The protein was pelleted by centrifugation for 10 min at 14 500*g*. The acetone was removed, and the protein pellet was resuspended in a 25 μL sample resuspension buffer (8 M urea, 2 M thiourea, 0.1 M Tris−HCl (pH 8.0) dissolved in HPLC-grade dH_2O). An aliquot (2 μL) was removed from each sample and quantified using the Qubit quantification system (Invitrogen), following the manufacturer's instructions. Ammonium bicarbonate (50 mM) (105 μL) was added to the remaining 20 μL of each sample. The protein sample was reduced by adding 1 μL of 0.5 M dithiothreitol (DTT) prepared 50 mM ammonium bicarbonate and incubated at 56 °C for 20 min, followed by alkylation with 0.55 M iodoacetamide, prepared 50 mM ammonium bicarbonate, at room temperature in the dark for 15 min. Protease Max surfactant trypsin enhancer (Promega) (1 μL of a 1% w/v solution dissolved in 50 mM ammonium bicarbonate) and 0.5 μg/μL of sequence grade trypsin (Promega) were added to each protein sample (80 μg) to give a ratio of 160:1 protein/trypsin. The protein/trypsin mixture was incubated at 37 °C for 18 h, after which digestion was terminated by adding 1 μL of 100% trifluoroacetic acid (TFA) to each tryptic digest sample and incubated at room temperature for 5 min. Samples were centrifuged for 10 min at 14 500*g*, and a volume equivalent to 30 μg of predigested protein was removed and purified for mass spectrometry using C18 Spin Columns (Pierce), following the manufacturer's instructions. The eluted peptides were dried using a SpeedyVac concentrator (Thermo Scientific Savant DNA120) and resuspended in 2% v/v acetonitrile and 0.05% v/v TFA to give a final peptide concentration of 1 μg/μL. The samples were sonicated for 5 min to aid peptide resuspension, followed by centrifugation for 5 min at 14 500*g*. The supernatant was removed and used for mass spectrometry.

Mass Spectrometry

The digested sample (1 μg) was loaded onto a Q-Exactive (ThermoFisher Scientific) high-resolution accurate mass spectrometer connected to a Dionex UltiMate 3000 (RSLCnano) chromatography system. Peptides were separated by an increasing acetonitrile gradient on a BioBasic C18 Picofrit column (100 mm length, 75 mm inner diameter), using a 120 min reverse-phase gradient at a flow rate of 250 nL/min. All data were acquired with the mass spectrometer operating in an automatic-dependent switching mode. A full MS scan at 140 000 resolution and a range of 300−1700 m/z was followed by an MS/MS scan at 17 500 resolution, with a range of 200−2000 m/z to select the 15 most intense ions prior to MS/MS.

Protein quantification and LFQ normalization of the MS/MS data were performed using MaxQuant version 1.5.3.3 (http://www.maxquant.org) following the general procedures and settings outlined in Hubner et al.[35] The Andromeda search algorithm incorporated in the MaxQuant software was used to correlate MS/MS data against the Uniprot-SWISS-PROT database for *Homo sapiens*, *A. fumigatus Af*293, and *P. aeruginosa* PAO1 (downloaded 16/09/2016; 55651 entries). The following search parameters were used: a first search peptide tolerance of 20 ppm, a second search peptide tolerance of 4.5 ppm with cysteine carbamidomethylation as a fixed modification and N-acetylation of protein and oxidation of methionine as variable modifications and a maximum of two missed cleavage sites allowed. False discovery rate (FDR) was set to 1% for both peptides and proteins, and the FDR was estimated following searches against a target−decoy database. Peptides with a minimum length of seven amino acids were considered for identification, and proteins were only considered identified when observed in three replicates of one sample group.

Data Analysis

P. aeruginosa CFU counts were compared via Student's *t* tests to determine statistical significance. *p*-values <0.05 were considered significant. The percentage change in the number of bacterial CFUs was calculated and $\log_{10}$-transformed. These results were analyzed using GraphPad Prism 5.

Perseus v.1.5.5.3 (www.maxquant.org/) was used for data analysis, processing, and visualization. Normalized LFQ intensity values were used as the quantitative measurement of protein abundance for subsequent analysis. The data matrix was first filtered for the removal of contaminants and peptides identified by site. LFQ intensity values were $\log_2$-transformed, and each sample was assigned to its corresponding group, i.e., *A. fumigatus*-exposed A549 cells versus the control (unexposed cells), *P. aeruginosa*-exposed A549 cells versus the control, and sequential infection versus the control. Proteins not found in three out of three replicates in at least one group were omitted from the analysis. A data-imputation step was conducted to replace missing values with values that simulate signals of low abundant proteins chosen randomly from a distribution specified by a downshift of 2 times the mean standard deviation (SD) of all measured values and a width of 0.3 times this SD.

Normalized intensity values were used for a principal component analysis (PCA). Exclusively expressed proteins (those that were uniquely expressed or completely absent in one group) were identified from the preimputation dataset and included in subsequent analyses. Gene ontology (GO) mapping was also performed in Perseus using the UniProt gene ID for all identified proteins to query the Perseus annotation file (downloaded October 2016) and extract terms for biological process, molecular function, and Kyoto Encyclopaedia of Gene and Genome (KEGG) name. Proteins

DOI: 10.1021/acs.jproteome.9b00520
J. Proteome Res. 2020, 19, 279−291

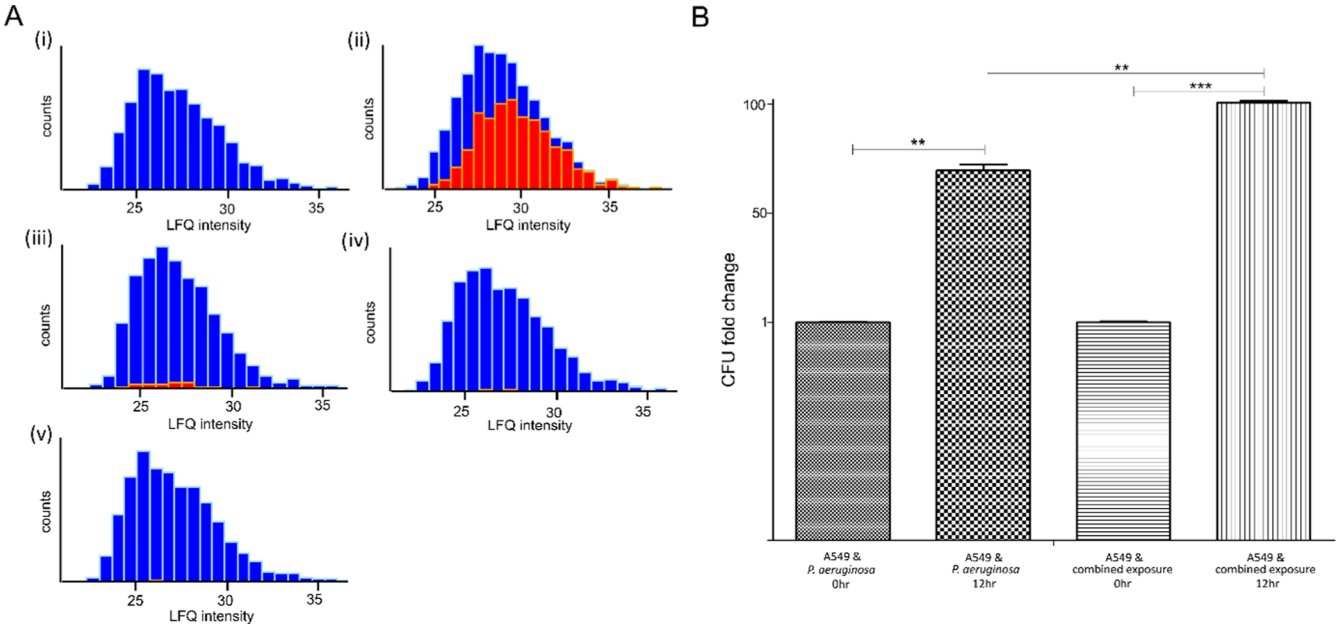

Figure 1. (A) Histograms (i–v) of $\log_2$-transformed LFQ intensity values displaying the proportion of *P. aeruginosa* proteins (red) present in representative samples comprising A549 proteins (blue). Bacterial proteins were not present in unexposed A549 cells (i). 41% of the total number of proteins identified were of bacterial origin after A549 cells were exposed to *P. aeruginosa* and *A. fumigatus* for 12 h (ii). 3.1% of the total number of proteins identified were of bacterial origin where A549 cells were exposed to *P. aeruginosa* for 12 h (iii). 0.26% of the total number of proteins identified were of bacterial origin where A549 cells were exposed *A. fumigatus* for 8 h and *P. aeruginosa* for 4 h (iv) or *P. aeruginosa* for 4 h (v). (B) A549 cells were incubated with *P. aeruginosa* (P.a.) or with *P. aeruginosa* and *A. fumigatus* (P.a. and A.f.) for 12 h. A CFU count performed on aliquots taken from the cultures before incubation (0 h) and 12 h post incubation revealed a 78-fold increase in the rate of bacterial replication where *P. aeruginosa* was cocultured with *A. fumigatus* than on its own. $*p < 0.05$, $**p < 0.01$, $***p < 0.001$; ns: not significant.

of nonhuman origin (i.e., with Uniprot IDs for *A. fumigatus* or *P. aeruginosa*), of which there were six, were removed from further analysis.

To visualize differences between two samples, pairwise Student's *t* tests were performed for all using a cutoff of $p < 0.05$ on the postimputated dataset. Volcano plots were generated in Perseus by plotting negative log *p*-values on the *y* axis and $\log_2$ fold change values on the *x* axis for each pairwise comparison. The "categories" function in Perseus was utilized to highlight and visualize the distribution of various pathways and processes on selected volcano plots. Statistically significant [analysis of variance (ANOVA), $p < 0.05$] and differentially abundant proteins (SSDA), i.e., with a fold change of ±1.5, were chosen for further analysis. An analysis of variance (ANOVA) was performed for multiple samples across all four groups using a permutation-based false discovery rate (FDR) of 5% and below to indicate statistically significant differentially abundant (SSDA) proteins. The $\log_2$-transformed LFQ intensities for all SSDA proteins were *z*-score-normalized and used for the hierarchical clustering of samples and SSDA proteins using Euclidean distance and average linkage.

GO and KEGG term enrichment analyses were performed on the major protein clusters identified by hierarchical clustering using Fisher's exact test (a Benjamini–Hochberg corrected FDR of 4%) for enrichment in Uniprot keywords, gene ontology biological process, gene ontology cellular component (CC), and KEGG (FDR < 4%). The Search Tool for the Retrieval of INteracting Genes/Proteins (STRING)[36] v10 (http://string-db.org/) was used to map known and predicted protein/protein interactions. UniProt gene lists (extracted from Perseus) were inputted and analyzed in STRING using the high confidence (0.700) setting to produce interactive protein networks for each group in all comparisons. GO term enrichment analyses for biological process, molecular function, and cellular compartment were then conducted to identify potential pathways and processes that warranted further analysis. Such pathways were examined using the KEGG pathway analysis (http://www.kegg.jp/kegg/tool/map_pathway2.html) using the "KEGG Mapper—SearchandColor Pathway" tool. The equivalent KEGG identifiers were obtained using the UniProt "Retrieve/ID mapping" function (http://www.uniprot.org/uploadlists/) with the organism set to *H. sapiens* (hsa). Retrieved KEGG IDs were used to identify the most represented pathways. The MS proteomics data and MaxQuant search output files have been deposited to the ProteomeXchange Consortium[37] via the PRIDE partner repository with the dataset identifiers PXD014022 (sequential exposure experiments) and PXD014535 (12 h coexposure and *P. aeruginosa* 12 h exposure experiments).

RESULTS

Label-free quantitative (LFQ) proteomics was performed on A549 cells exposed to *P. aeruginosa* and a coculture of *P. aeruginosa* and *A. fumigatus* for 12 h. Data analysis revealed that a significant proportion (40.7%) of the proteins identified in coculture samples were of bacterial origin, while the abundance of bacterial proteins detected in the samples treated with *P. aeruginosa* only was far less (63/2099 proteins detected; 3.1%). Histograms were generated based on $\log_2$-transformed LFQ intensity values for all identified proteins in Perseus to determine the distribution of the data. The high frequency of bacterial protein abundance observed in the coculture samples (Figure 1A-ii) compared to that of the samples treated with *P. aeruginosa* only (Figure 1A-iii) was indicative of the increase in

DOI: 10.1021/acs.jproteome.9b00520
J. Proteome Res. 2020, 19, 279–291

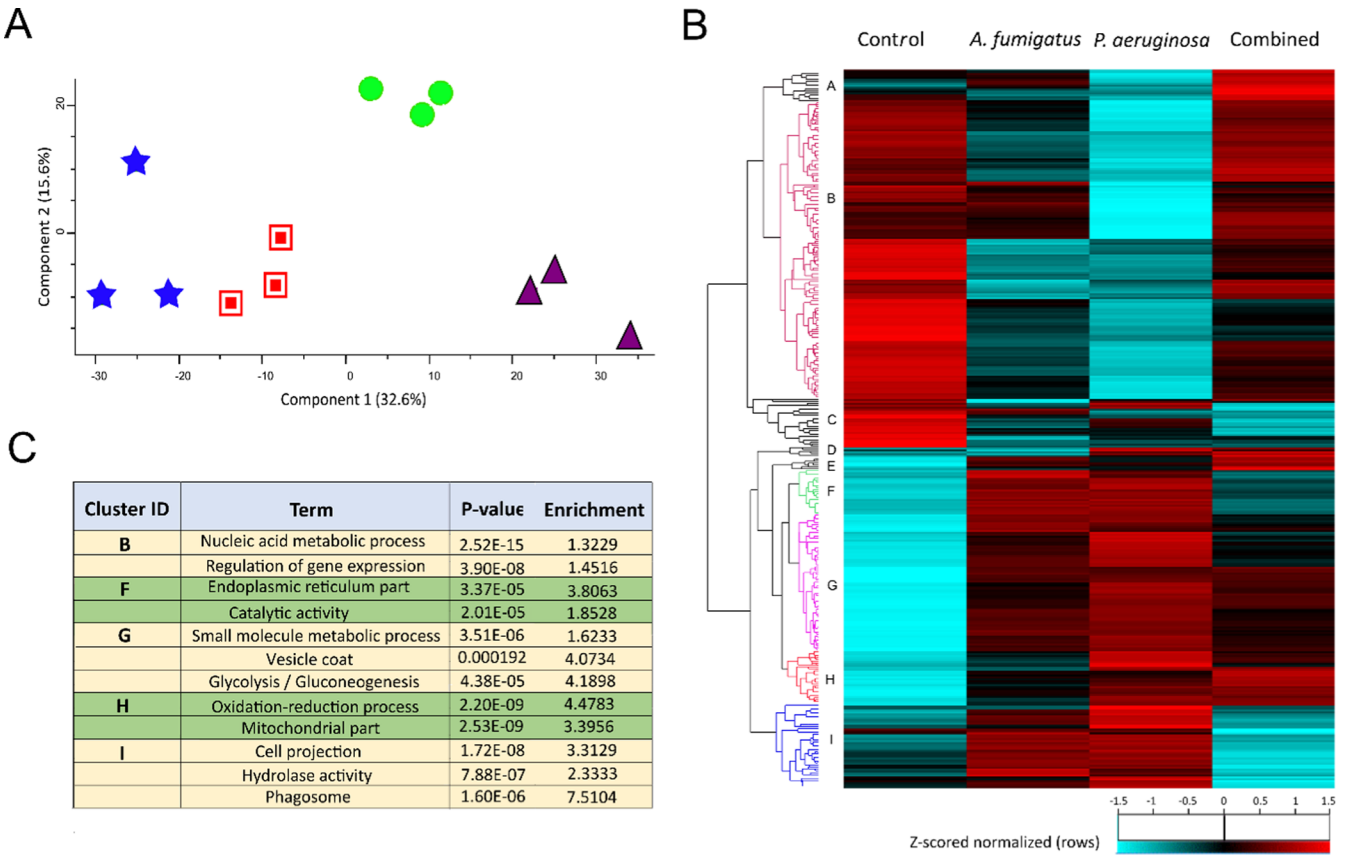

C

Cluster ID	Term	P-value	Enrichment
B	Nucleic acid metabolic process	2.52E-15	1.3229
	Regulation of gene expression	3.90E-08	1.4516
F	Endoplasmic reticulum part	3.37E-05	3.8063
	Catalytic activity	2.01E-05	1.8528
G	Small molecule metabolic process	3.51E-06	1.6233
	Vesicle coat	0.000192	4.0734
	Glycolysis / Gluconeogenesis	4.38E-05	4.1898
H	Oxidation-reduction process	2.20E-09	4.4783
	Mitochondrial part	2.53E-09	3.3956
I	Cell projection	1.72E-08	3.3129
	Hydrolase activity	7.88E-07	2.3333
	Phagosome	1.60E-06	7.5104

Figure 2. (A) Principal component analysis (PCA) of untreated A549 cells (triangles), A549 cells treated with *P. aeruginosa* (stars), and *A. fumigatus* (squares) or sequential exposure to both pathogens (circles). A clear distinction can be observed between each of the treated groups and the control. (B) Clusters based on protein abundance profile similarities were resolved by hierarchical clustering of multisample comparisons between the four sample groups of A549 cells. Nine clusters (A−I) were resolved comprising proteins that display similar expression profiles across treatments. Of these, five clusters (B, F−I) had statistically enriched gene ontology and KEGG terms associated with them (Dataset S2B), and the main terms are summarized for each in (C).

replication that occurs when *P. aeruginosa* was cocultured with *A. fumigatus*. To validate this finding, colony-forming unit (CFU) counts were performed on samples taken from the A549 cell cultures, in the presence or absence of *A. fumigatus*. There was a 78-fold increase in bacterial replication where *P. aeruginosa* was incubated with *A. fumigatus* and A549 cells compared to that found when *P. aeruginosa* was incubated with A549 cells alone (Figure 1B).

To assess the effect on bacterial growth in the absence of A549 cells, *P. aeruginosa* was cultured for 12 h on its own or in coculture with *A. fumigatus* conidia. Where *A. fumigatus* conidia were present, *P. aeruginosa* growth had increased by 5-fold (as measured by CFU counts) compared to the cultures that did not contain conidia (Figure S1A, Supporting Information). To investigate whether the presence of *A. fumigatus* conidia was required to induce bacterial growth proliferation or if the secretome of the fungus having being exposed to *P. aeruginosa* was sufficient to do so, *P. aeruginosa* was incubated for 12 h in the supernatant of a 12 h coculture of *A. fumigatus* and *P. aeruginosa* and in the supernatant of a 12 h *P. aeruginosa* culture. CFU counts performed after 12 h revealed no growth-promoting effect on the bacteria incubated with the supernatant from the coculture (Figure S1B), suggesting that *A. fumigatus* conidia must be present to promote bacterial growth.

To determine the time point at which exponential growth began in the presence of *A. fumigatus*, CFU counts were performed at 2 h time intervals from cultures of *P. aeruginosa* in the absence and presence of *A. fumigatus*. The results suggested that by 4 h, the rate of bacterial replication began to increase rapidly when cocultured in the presence of *A. fumigatus* (Figure S1C).

Based on these results, A549 cells were exposed to *A. fumigatus* for 8 h, followed by *P. aeruginosa* for 4 h, and the proteomic response was compared to that of A549 cells exposed to *A. fumigatus* or *P. aeruginosa* alone. The proportion of bacterial proteins detected in the A549 cells exposed to *A. fumigatus* and *P. aeruginosa* sequentially for 8 and 4 h, respectively, was 0.26% (Figure 1A-iv,v). In total, 4048 proteins were identified initially, of which 2264 remained after filtering and processing (Dataset S1A, Supporting Information). Of the 2264 proteins identified post imputation, 285 proteins in the *A. fumigatus*-exposed group (Dataset S1B), 495 proteins in the *P. aeruginosa*-exposed group (Dataset S1C), and 252 proteins in the sequentially exposed group (Dataset S1D) were determined to be statistically significant ($p < 0.05$) differentially abundant (SSDA) with a fold change of ±1.5. Arising from comparisons made between the sequentially exposed groups and *A. fumigatus*-exposed groups, 156 SSDA proteins were detected (Dataset S1E). Arising from comparisons made between the sequentially exposed groups and *P. aeruginosa*-exposed groups, 302 SDDA proteins were detected (Dataset S1F). SSDA proteins identified from pairwise *t*-tests were searched against the STRING and KEGG databases and

DOI: 10.1021/acs.jproteome.9b00520
J. Proteome Res. 2020, 19, 279−291

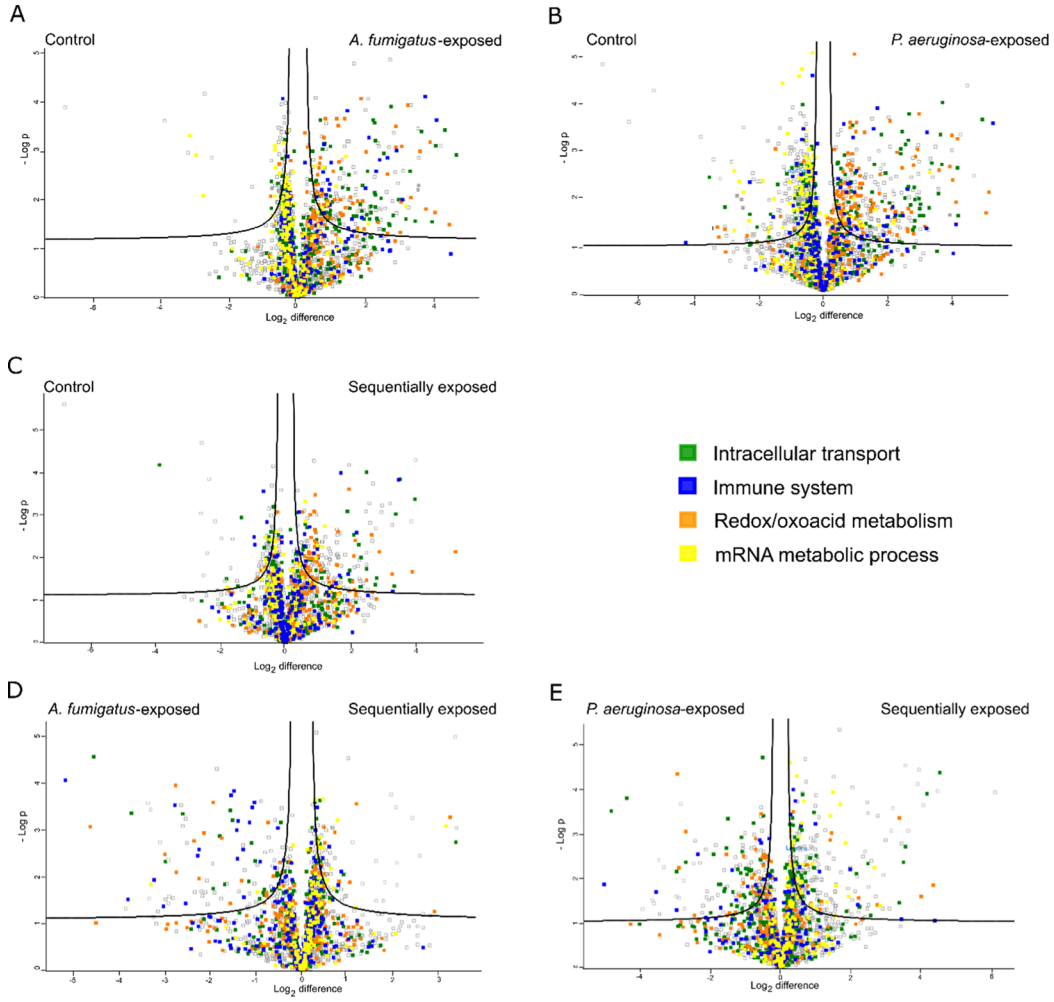

Figure 3. Volcano plots derived from pairwise comparisons between A549 cells and (A) *A. fumigatus*-exposed A549 cells, (B) *P. aeruginosa*-exposed A549 cells, and (C) sequentially exposed A549 cells and between sequentially exposed A549 cells and (D) *A. fumigatus*-exposed A549 cells and (E) *P. aeruginosa*-exposed A549 cells. Distribution of quantified proteins according to *p*-value (−log 10 *p*-value) and fold change (log_2 mean LFQ intensity difference) is shown. Proteins above the line are considered statistically significant (*p*-value <0.05). Protein components of the immune system (blue) and of intracellular transport (green) were most abundant in all pathogen-exposed groups compared to those in the control. A greater immune response was observed in the *A. fumigatus*- and *P. aeruginosa*-exposed groups than in the sequentially exposed groups. Proteins associated with mitochondrial activity including redox reaction and oxacid metabolic processes (orange) were more abundant in pathogen-exposed groups compared to those in the control, but less abundant in sequentially exposed groups when compared to those in the *A. fumigatus*- and *P. aeruginosa*-exposed cells. A decrease in the relative abundance of proteins associated with RNA metabolic processes (yellow) was most evident in the *P. aeruginosa*-exposed cells although also observed to a lesser extent in the *A. fumigatus*- and sequentially exposed cells.

used to identify biological pathways and processes over-represented in a particular group (Figures S2A,C and S3A,M).

A principal component analysis (PCA) of all identified proteins resolved distinct differences between the proteomes of each group (Figure 2A). Components 1 and 2 accounted for 48.2% of the total variance within the data, and all replicates resolved into their corresponding samples. The control sample displayed a clear divergence to those that were challenged with *A. fumigatus* and/or *P. aeruginosa*. A distinct difference was also observed between the sequentially exposed A549 cells and cells exposed to *A. fumigatus* or *P. aeruginosa*.

Hierarchical clustering was performed on the *z*-scored normalized LFQ intensity values for the 618 SSDA proteins identified (ANOVA; Benjamini−Hochberg procedure, FDR cutoff value of ≤0.05). All three biological replicates resolved into their respective samples. Nine (A−I) protein clusters based on protein abundance profile similarities (Figure 2B) were also resolved. GO and KEGG term enrichment analyses were performed on all protein clusters. Five clusters had enriched terms (clusters B, F−I; Figure S2B), and each cluster had a representative process or pathway characteristic to that group (Figure 2C). These included RNA metabolic processing (cluster B), protein processing (cluster F), carbon metabolism (cluster G), mitochondrial processes (cluster H), and pathogen uptake and processing (cluster I). Details of all clusters are included in the Dataset S2A,B.

Within cluster B (Figure 2C), GO terms and KEGG pathway analysis resolved 256 proteins with terms associated with RNA processes including gene expression, posttranscriptional regulation, mRNA splicing, translation initiation, ribosomes, and transport. Proteins involved in these processes were distinctly less abundant in the *P. aeruginosa*-exposed A549 cells as compared to those in the other groups, indicating the attenuation of mRNA processing and translational machinery in A549 cells treated with the bacteria only. Proteins present in cluster F (Figure 2C) were primarily involved with protein

DOI: 10.1021/acs.jproteome.9b00520
J. Proteome Res. 2020, 19, 279−291

modifications, protein folding, protein degradation, and export from the endoplasmic reticulum (ER). The relative abundance of proteins associated with protein processing in the ER was greater in the *A. fumigatus*- and *P. aeruginosa*-exposed A549 cells compared to that of the sequentially infected group and the controls. This trend was reflected in the KEGG pathway analysis (Figure S3F). The relative abundance of proteins involved in protein trafficking and vesicle-mediated transport was higher in all infection groups compared to that of the control (Figure 2C, cluster G). These processes are also highlighted as being increased in the images derived from the STRING network analysis (Figure S2A−C) and are depicted in KEGG pathways (Figure S3I). Production of energy by carbohydrate and fatty acid metabolism, and energy derivation by oxidation was upregulated in the three infected groups compared to that of the control (Figure S3A−D, KEGG pathways). These pathways were most prominent in the *P. aeruginosa*-exposed group (Figure 2C, cluster G). Among the GO terms included in this cluster were oxoacid, cellular ketone, and carbohydrate metabolic processes and the KEGG glycolysis/gluconeogenesis pathway.

The relative abundance of mitochondrial proteins and mitochondria-related processes was increased across all three infected groups of A549 cells compared to that of the control (Figure 2C, cluster H). This is reflected in the KEGG pathways (Figure S3D,E). GO terms for the mitochondria and associated processes including mitochondrion, oxidoreductase activity, oxidative phosphorylation (OXPHOS), and the respiratory electron transport chain were included in this cluster. Proteins associated with these GO terms were most abundant in the *P. aeruginosa*-exposed group and sequentially infected group, respectively, compared to those in the *A. fumigatus*-exposed group and the control.

GO term enrichment analysis within cluster I (Figure 2C) identified key biological processes, molecular functions, and cellular components involved with the uptake and processing of pathogens and activation of an immune response. The protein abundance profile of the sequentially exposed groups was comparable to that of the control but distinctly different from that of the *A. fumigatus*- and *P. aeruginosa*-exposed groups in which the relative abundance of proteins was greater compared to that of the sequentially exposed A549 cells. Biological processes included cellular response to stimuli, cell motility, vesicle-mediated transport, and signal transduction. Catalytic activities involving hydrolases, pyrophosphatases, and nucleoside-triphosphatase were among the molecular functions included in this cluster. Proteins involved in parts of the cell that form cell projections, endosome, lysosome, and receptor complexes formed a significant proportion of the proteins found in this cluster. This trend was reflected in the KEGG maps (Figure S3I−M) where the levels of proteins in several pathways associated with pathogen uptake and processing including endocytosis, phagosome, and lysosome activity were reduced in the sequentially exposed groups.

Volcano plots were produced to determine the differences in protein expression between two samples and to depict the changes in pathways and processes of those proteins that are involved in (Figure 3A−E). Increases in mitochondrial-related processes, including oxidative phosphorylation and the tricarboxylic cycle (TCA) cycle, were observed in all pathogen-exposed groups, supporting the profile observed in the heatmap (Figure 2B, cluster H). Immune system processes and protein transport were increased in the *A. fumigatus*- and *P. aeruginosa*-exposed groups to a greater extent than those in the sequentially exposed cells (Figure 3B). A decrease in the relative abundance of proteins associated with RNA metabolic processes was most evident in the *P. aeruginosa*-exposed cells although this process was also observed to a lesser extent in the *A. fumigatus*- and sequentially exposed cells (Figures 3A−C and S2A−C). A similar trend in the downregulation of this pathway was observed in Figure 2B, cluster B.

To investigate the enzyme-driven pathways between the four groups of A549 cells, SSDA proteins were inputted into the KEGG mapping tool (Figure S3A−M). The relative abundance of proteins associated with carbon metabolism in the form of glycolysis and fatty acid degradation was increased in all treated groups (Figure S3A−C). Mitochondrial processes including the TCA cycle and oxidative phosphorylation pathways were upregulated in all groups compared to those in the control (Figures S2A−C and S3B−E). Pathway analysis performed between the *A. fumigatus*- and *P. aeruginosa*-exposed and sequentially exposed groups revealed distinct differences between the different infection treatments. The relative abundance of proteins involved in pathways associated with protein processing in the endoplasmic reticulum, endocytosis, regulation of the actin cytoskeleton, bacterial invasion of epithelial cells, the phagosome, and lysosome was increased in the *A. fumigatus*- and *P. aeruginosa*-exposed cells compared to that in the controls and the sequentially infected cells (Figure S3F−M). This indicates that when A549 cells were exposed to these pathogens sequentially, these pathways were inactive.

All SSDA proteins identified in A549 cells following exposure of *A. fumigatus* are listed in Dataset S1B. The top three proteins with the greatest increase in relative abundance were leucine-rich pentatricopeptide repeat motif-containing protein, mitochondrial (25.1-fold), fatty acid synthase (21.5-fold), and dolichyl-diphosphooligosaccharide (19.7-fold). Proteins with the greatest decrease in relative abundance included heat shock 70 kDa protein 6 (114.1-fold), Catenin α-2 (15.1-fold), and PIH1 domain-containing protein 1 (9.3-fold).

All SDDA proteins detected in A549 cells following exposure to *P. aeruginosa* are presented in Dataset S1C. The top three proteins with the greatest increase in relative abundance were cytoplasmic dynein 1 heavy chain 1 (38.5-fold), ADP/ATP translocase 2 (35.5-fold), and fatty acid synthase (33.4-fold). Proteins with the greatest decrease in relative abundance included heat shock 70 kDa protein 6 (114.4-fold), acyl-CoA-binding protein (65.8-fold), and cellular nucleic-acid-binding protein (38.3-fold).

All SSDA proteins detected in the sequentially exposed groups are presented in Dataset S1D. The top three proteins with the greatest increase in relative abundance were ADP/ATP translocase 2 (37-fold), eukaryotic translation initiation factor 3 subunit L (15.9-fold), and dolichyl-diphosphooligosaccharide (15.8-fold). Proteins with the greatest decrease in relative abundance included heat shock 70 kDa protein 6 (112.1-fold), ras-related protein Rab-5C (14.7-fold), and coiled-coil domain-containing protein 12 (6.1-fold).

DISCUSSION

The complex nature of the polymicrobial environment that occupies the CF lung lends to the difficulties associated with understanding the dynamics between the various microorganisms that contribute to chronic infection within the lung.[38] Recent molecular culture-independent techniques have

DOI: 10.1021/acs.jproteome.9b00520
J. Proteome Res. 2020, 19, 279−291

revealed the existence of a diverse microbial community in the CF lung.[39,40] In addition to *Burkholderia cepacia*, it is widely accepted that *P. aeruginosa* predominates as the primary bacterial pathogen of the CF lung from the second decade of life onwards.[2,41] *A. fumigatus* exists as the most common fungal pathogen associated with the CF airways, and while it is responsible for the onset of an allergic bronchopulmonary response (e.g., ABPA), it rarely becomes invasive.[5]

While many studies have investigated the response of a host to a single pathogen, few have examined the response of the host to coinfection by more than one pathogen. This study aimed to characterize, for the first time, the whole-cell proteomic response of A549 cells, an in vitro model of the alveolar epithelium, to sequential exposure by *A. fumigatus* and *P. aeruginosa*, and to understand why *P. aeruginosa* ultimately predominates as the primary pathogen. Initial findings of pilot proteomic experiments revealed that the rate of bacterial replication increased when *A. fumigatus* conidia were cocultured with *P. aeruginosa*. This was reflected in the high abundance of bacterial proteins detected by the mass spectrometer where *A. fumigatus* was present compared to when *P. aeruginosa* was cultured with A549 cells alone for the same length of time. CFU counts confirmed the finding observed in the proteomics data and determined that *A. fumigatus* conidia must be present for bacterial replication to escalate, as the secretome from a coculture of *A. fumigatus* and *P. aeruginosa* did not induce the same growth effect.

Having determined the point at which *P. aeruginosa* began to replicate exponentially in the presence of *A. fumigatus*, the whole-cell proteomic response of A549 cells to sequential infection with *A. fumigatus* and *P. aeruginosa* was characterized. LFQ proteomics was used to compare the individual proteins and pathways, which contribute to the response of A549 cells when exposed to *A. fumigatus* or *P. aeruginosa* with those observed in the sequentially exposed A549 cells. Based on the analysis of the proteomic profile, distinct similarities and differences were observed between the three infection groups. These findings may explain why *P. aeruginosa* predominates in the presence of *A. fumigatus*.

Exposure to *A. fumigatus* and/or *P. aeruginosa* Increases Energy Output in A549 Cells

Host cells respond to the presence of pathogens by altering their metabolic processes,[42] and a clear signature of microbial infection is an alteration in carbohydrate and amino acid metabolism by the host.[43] In this study, comparative analysis between the control and the three infection models demonstrated a clear increase in the relative abundance of proteins associated with carbohydrate and amino acid metabolism. An increase in host metabolic processes was greatest in the *P. aeruginosa*-exposed A549 cells, suggesting that *P. aeruginosa* induces a more drastic alteration to host cell energy metabolism than that induced by *A. fumigatus*.

Exposure to *A. fumigatus* and/or *P. aeruginosa* Induces Mitochondrial Stress in A549 Cells

Reactive oxygen species (ROS) such as superoxide anion (O_2^-) or hydrogen peroxide (H_2O_2) are byproducts of energy metabolism and β-oxidation of fatty acids that occur in the mitochondria. Excessive levels of ROS induce oxidative stress. This is an indicator of mitochondrial dysfunction, often associated with diseases such as Huntington's disease.[44] ROS are key components of the innate immune response, and production is intensified during microbial infection whereby it is directly and indirectly involved in combating infectious agents through the direct killing of the pathogen and by activating inflammatory pathways, respectively.[45] In this study, processes relating to oxidative stress, including fatty acid degradation and the TCA cycle, the OXPHOS pathway and Huntington's disease pathway, were enriched across all treated groups of A549 cells. The abundance of proteins associated with the mitochondrial activity, as determined by hierarchical clustering, was greatest in the *P. aeruginosa*- and sequentially treated cells compared to that of the *A. fumigatus*-treated cells. These results indicate that *P. aeruginosa* is the cause of the heightened oxidative stress response observed in the sequentially exposed A549 cells. The redox-reactive phenazine, pyocyanin (PCN), is produced by most strains of *P. aeruginosa*, including PAO1,[46] and can induce oxidative stress in epithelial cells.[47,48] Its effect on the decline of respiratory health and lung function in CF is well documented, and PCN-overproducing strains have been isolated from the CF airways.[48−51]

Aside from the immune response, few studies have focused on the effect of *A. fumigatus* on mammalian cells, and in the context infection, more is known about the host response to *P. aeruginosa*. In this study, an increase in the relative abundance of proteins and pathways associated with the mitochondria in the *A. fumigatus*-exposed A549 cells indicates that *A. fumigatus* induces mitochondrial stress in the host. However, this response is somewhat less intense than that caused by *P. aeruginosa*. One consequence of mitochondrial stress is apoptosis, which can be activated in response to stress-induced danger signals, such as microbial infection.[52,53] Several studies have demonstrated that *A. fumigatus* can inhibit apoptosis in epithelial cells and thus survive and germinate in the host, evading detection by the immune system.[34,53−55] The results here show that a number of pathways associated with mitochondrial stress were not increased to the same extent in the *A. fumigatus*-exposed A549 cells as observed in the *P. aeruginosa*- and sequentially exposed cells.

Exposure to *A. fumigatus* or *P. aeruginosa* Reduces Ribosomal Activity in A549 Cells

Microbial pathogens can influence and manipulate the host environment by targeting host translational machinery in an attempt to limit the translation of mRNAs that code for immune effectors. Translation inhibition alerts the host to infection, which may respond by increasing the activity of posttranscriptional mediators required to meet the demands of orchestrating an appropriate immune response.[56−60] In this study, the levels of proteins associated with mRNA processing were significantly lower in the *P. aeruginosa*-exposed A549 cells compared to those in the control and the other infection groups.

A. fumigatus has evolved mechanisms to evade the host immune response, and some of the molecular components involved in immune recognition and evasion have been reported.[34,55] Given that translational inhibition can activate the immune response, noninterference with protein synthesis may be an adaption, which enables *A. fumigatus* to avoid triggering the host immune system. Interestingly, the exposure of A549 cells to *P. aeruginosa*, subsequent to *A. fumigatus*, did not appear to affect translational processing. By maintaining regular protein synthesis in the host, it is possible that *A. fumigatus* creates an environment in which *P. aeruginosa* can also avoid triggering an immune response, allowing the pathogen time to establish infection. These findings may

DOI: 10.1021/acs.jproteome.9b00520
J. Proteome Res. 2020, 19, 279−291

provide one explanation as to why the proteomic response of A549 cells to sequential exposure of *A. fumigatus* and *P. aeruginosa* resembles that of the fungal infection and not of the bacterial infection.

Exposure to *A. fumigatus* and/or *P. aeruginosa* Alters Protein Processing Activity in the ER

Microbial infection increases the demand for the biosynthesis and folding of inflammatory proteins. This can induce a stress response in the endoplasmic reticulum (ER), known as the unfolded protein response (UPR), which is caused by a buildup of misfolded or unfolded proteins in the ER lumen.[61] ER stress and UPR activation result in the upregulation of a number of pathways observed in this study, including the attenuation of mRNA translation, increased protein folding, and degradation of permanently misfolded proteins by the proteasome via the ER-associated degradation pathway.[62]

In vivo and in vitro studies have demonstrated an increase in ER stress markers in murine lungs and tracheal epithelial cells challenged with *A. fumigatus* antigens, respectively, and it has recently been suggested that ABPA-related symptoms may be attributed to the *A. fumigatus*-induced ER stress.[63,64] *P. aeruginosa* secretes virulence factors including PCN and TpIE that are known to induce ER stress and activate UPR via the p38 mitogen-activated protein kinase (MAPK) pathway.[61,65,66] The relative abundance of multiple proteins associated with protein processing in the ER was increased in the *A. fumigatus*- and *P. aeruginosa*-exposed groups compared to that in the controls and sequentially exposed A549 cells. These included proteins involved in cotranslational and posttranslational modifications, protein folding, protein transport from the ER, members of the translocon-associated protein complex, and regulators of ER-stress-induced apoptosis. The p38 MAPK signaling pathway is central to integrating the ER stress response and the immune response to *P. aeruginosa* infection.[64,67,68] Our data revealed a significant increase in the levels of multiple proteins associated with the MAPK pathway in both the *A. fumigatus*- and *P. aeruginosa*-exposed A549 cells compared to that in the sequentially exposed cells and the controls. Based on these findings, *A. fumigatus* and *P. aeruginosa* are more likely to induce ER stress and consequently ER-stress-induced inflammation in A549 cells exposed to the cells separately than sequentially. This response, or lack thereof, in the sequentially exposed cells may influence the way in which the host challenges the pathogen.

P. aeruginosa Downregulates the Ubiquitination Pathway in A549 Cells

A decrease in the relative abundance of several proteins associated with ubiquitin-mediated proteolysis was identified in the *P. aeruginosa*-exposed and sequentially exposed cells, indicating a role for *P. aeruginosa* in altering the protein degradation pathway. Ubiquitin-dependent proteasomal degradation and ubiquitin-associated autophagy play a central role during and post pathogen-induced infection by eliminating misfolded, damaged, or short-lived regulatory proteins.[69,70] These pathways are crucial in maintaining protein homeostasis, as sustained inflammation has detrimental outcomes for host tissue. Some pathogens, including *P. aeruginosa*, have evolved mechanisms to interfere with elements of the host ubiquitination system, which alter the host cell proteome and allow pathogens to evade the immune response.[71−73]

Exposure to *A. fumigatus* or *P. aeruginosa* Induces an Immune Response in A549 Cells

The proteomic analysis in this study showed that *A. fumigatus* and *P. aeruginosa*, separately and sequentially, activated an immune response in A549 cells. Compared to the *A. fumigatus*-exposed cells, the relative abundance of many immune system proteins in the sequentially exposed group was decreased. This suggests that certain elements of the immune response are downregulated by *P. aeruginosa* but not by *A. fumigatus*. Thus, the immune response of A549 cells when exposed to *A. fumigatus* or *P. aeruginosa* is distinctly different from that when cells are exposed to these pathogens sequentially. This may be due to the initial activation of the immune system caused by *A. fumigatus*, which is subsequently attenuated by the presence of *P. aeruginosa*. This is not entirely surprising as there is evidence to show that virulence factors secreted by some pathogenic bacteria, including *P. aeruginosa*, can inhibit elements of the immune system from activating a proinflammatory response.[74−76]

Sequential Exposure to *A. fumigatus* and *P. aeruginosa* Interferes with Actin Formation and Pathogen Processing in A549 Cells

The relative abundance of proteins associated with endocytosis and the actin cytoskeleton was increased in the *A. fumigatus*- and *P. aeruginosa*-exposed A549 cells in comparison to that of the control groups and sequentially exposed cells. This indicates that A549 cells are capable of initiating phagocytosis when exposed to *A. fumigatus* or *P. aeruginosa*; however, sequential exposure to both pathogens appears to interfere with this process. Although *A. fumigatus* and *P. aeruginosa* can be internalized by, and trafficked within, A549 cells, these pathogens can also inhibit phagocytosis through various mechanisms.[28,30,31,33,34,77−83]

Once internalized, pathogens become engulfed in phagosomes, and these vacuoles become progressively more acidified by vATPases, until they fuse with a lysosome to form phagolysosomes, an acidified vacuole that is characterized by degradative enzyme activity and the production of ROS.[84] *A. fumigatus* and *P. aeruginosa* can survive and replicate within A549 cells by interfering with the acidification of phagosomes and hijacking proteins involved in vesicle trafficking.[28,30,31,34,85,86] Our study determined that the relative abundance of proteins involved in the phagosomal and lysosomal pathways was greater in the fungal- and bacterial-exposed A549 cells in comparison to that of the control and sequentially exposed cells. However, the relative abundance of vATPase was increased in the *P. aeruginosa*- and sequentially exposed A549 cells, indicating that *P. aeruginosa* was responsible for increases to the levels of this protein. Taken together, these results indicate that A549 cells respond to infection by *A. fumigatus* or *P. aeruginosa* by initiating phagocytosis and pathogen degradation pathways, whereas when challenged with both pathogens sequentially, the host cell seems unable to activate a similar response. The altered response appears to begin with exposure to *A. fumigatus*, which programs the behavior of the host cell such that its response to *P. aeruginosa* becomes compromised. In the context of CF, *A. fumigatus*-mediated alterations to the host epithelia may compromise the ability of pulmonary epithelial cells to respond adequately to subsequent infection by *P. aeruginosa*, thereby enabling these bacteria to bypass frontline defenses in the pulmonary immune system and proliferate. The proteomic

DOI: 10.1021/acs.jproteome.9b00520
J. Proteome Res. 2020, 19, 279−291

data generated in this study may help to explain why, in the CF airways, coinfection by *A. fumigatus* and *P. aeruginosa* results in a worse diagnosis than infection by either pathogen alone.[87−91]

CONCLUSIONS

In this work, the proteomic response of A549 cells to *A. fumigatus* and *P. aeruginosa* revealed novel insights into the molecular responses to sequential infection of both pathogens. These findings may have significant clinical relevance to CF patients. The results highlight a specific series of proteomic responses when cells were exposed to a single pathogen including the inhibition of translation, infection-mediated protein processing in the ER, and upregulation of the immune response. In contrast, initially exposing cells to *A. fumigatus* and then to *P. aeruginosa* lead to an intrinsically different response characterized by the inhibition of phagocytosis and the pathogen degradation pathway involving phagosome and lysosome. In the lungs of CF patients, pathogens such as *A. fumigatus* and *Staphylococcus aureus* predominate in the early years of life, but *P. aeruginosa* and *Burkholderia* become the dominant pathogens in the later years of life and contribute to death. The results presented here suggest that pre-exposure to *A. fumigatus* alters the response of cells to *P. aeruginosa* exposure, increasing host susceptibility to colonization by bacteria. The inability of host cells to respond adequately to bacterial infection may lead to the increased development of disease symptoms in vivo. This indicates that in the lungs of CF patients, *A. fumigatus* may promote, in part, the colonization of the CF lung by *P. aeruginosa*.

ASSOCIATED CONTENT

Supporting Information

The Supporting Information is available free of charge on the ACS Publications website at DOI: 10.1021/acs.jproteome.9b00520.

Images comparing the fold changes in *P. aeruginosa* replication in the presence and absence of *A. fumigatus* (Figure S1A−C); selection of images from the STRING interaction network analysis of SSDA proteins identified in pairwise t-tests (Figure S2A−C); selection of KEGG pathways for SSDA proteins identified in pairwise *t*-tests (Figure S3A−M) (PDF)

All proteins identified from control-exposed, *A. fumigatus*-exposed, *P. aeruginosa*-exposed, and sequentially exposed A549 cells and statistically significantly differentially abundant proteins (two-sample *t*-tests; $p < 0.05$) for pairwise comparisons (Dataset S1A−F) (XLSX)

Proteins and enriched terms associated with clusters A−I resolved by hierarchical clustering (Dataset S2A,B) (XLSX)

AUTHOR INFORMATION

Corresponding Author

*E-mail: kevin.kavanagh@nuim.ie. Phone: +353-1-708 3859. Fax: +353-1-708 3845.

ORCID

Kevin Kavanagh: 0000-0003-3186-0292

Notes

The authors declare no competing financial interest.

ACKNOWLEDGMENTS

A.M. is the recipient of an Irish Research Council Doctoral scholarship. Q-Exactive mass spectrometer was funded under the SFI Research Infrastructure Call 2012, Grant Number: 12/RI/2346 (3).

LIST OF ABBREVIATIONS

ABPA, allergic bronchopulmonary aspergillosis; CC, cellular component; CF, cystic fibrosis; CFU, colony-forming units; ER, endoplasmic reticulum; FDR, false discovery rates; GO, gene ontology; LFQ, label-free quantitative; MAPK, mitogen-activated protein kinase; OXPHOS, oxidative phosphorylation; PCA, principal component analysis; PCN, pyocyanin; ROS, reactive oxygen species; SSDA, statistically significant differentially abundant; TCA, tricarboxylic cycle; UPR, unfolded protein response

REFERENCES

(1) Osherov, N. Interaction of the pathogenic mold *Aspergillus fumigatus* with lung epithelial cells. *Front. Microbiol.* **2012**, *3*, No. 346.

(2) Kassim, S. Y.; Gharib, S. A.; Mecham, B. H.; Birkland, T. P.; Parks, W. C.; McGuire, J. K. Individual matrix metalloproteinases control distinct transcriptional responses in airway epithelial cells infected with *Pseudomonas aeruginosa*. *Infect. Immun.* **2007**, *75*, 5640−5650.

(3) Harriott, M. M.; Noverr, M. C. Importance of Candida-bacterial polymicrobial biofilms in disease. *Trends Microbiol.* **2011**, *19*, 557−563.

(4) Filkins, L. M.; O'Toole, G. A. Cystic Fibrosis Lung Infections: Polymicrobial; Complex; and Hard to Treat. *PLoS Pathog.* **2015**, *11*, No. e1005258.

(5) Reece, E.; Segurado, R.; Jackson, A.; McClean, S.; Renwick, J.; Greally, P. Co-colonisation with *Aspergillus fumigatus* and *Pseudomonas aeruginosa* is associated with poorer health in cystic fibrosis patients: an Irish registry analysis. *BMC Pulm. Med.* **2017**, *17*, No. 70.

(6) Govan, J. R.; Deretic, V. Microbial pathogenesis in cystic fibrosis: mucoid *Pseudomonas aeruginosa* and *Burkholderia cepacia*. *Microbiol. Rev.* **1996**, *60*, 539−574.

(7) Koch, C. Early infection and progression of cystic fibrosis lung disease. *Pediatr. Pulmonol.* **2002**, *34*, 232−236.

(8) Goldberg, J. B.; Pier, G. B. The role of the CFTR in susceptibility to *Pseudomonas aeruginosa* infections in cystic fibrosis. *Trends Microbiol.* **2000**, *8*, 514−520.

(9) Parkins, M. D.; Somayaji, R.; Waters, V. J. Epidemiology, Biology, and Impact of Clonal *Pseudomonas aeruginosa* Infections in Cystic Fibrosis. *Clin. Microbiol. Rev.* **2018**, *4*, No. e00019-18.

(10) Goodman, A. L.; Kulasekara, B.; Rietsch, A.; Boyd, D.; Smith, R. S.; Lory, S. A signaling network reciprocally regulates genes associated with acute infection and chronic persistence in *Pseudomonas aeruginosa*. *Dev. Cell* **2004**, *7*, 745−754.

(11) Winstanley, C.; O'Brien, S.; Brockhurst, M. A. *Pseudomonas aeruginosa* Evolutionary Adaptation and Diversification in Cystic Fibrosis Chronic Lung Infections. *Trends Microbiol.* **2016**, *24*, 327−337.

(12) Breidenstein, E. B.; de la Fuente-Nunez, C.; Hancock, R. E. *Pseudomonas aeruginosa*: all roads lead to resistance. *Trends Microbiol.* **2011**, *19*, 419−426.

(13) Caldwell, C. C.; Chen, Y.; Goetzmann, H. S.; Hao, Y.; Borchers, M. T.; Hassett, D. J.; Young, L. R.; Mavrodi, D.; Thomashow, L.; Lau, G. W. *Pseudomonas aeruginosa* exotoxin pyocyanin causes cystic fibrosis airway pathogenesis. *Am. J. Pathol.* **2009**, *175*, 2473−2488.

(14) Stevens, D. A.; Moss, R. B.; Kurup, V. P.; Knutsen, A. P.; Greenberger, P.; Judson, M. A.; Denning, D. W.; Crameri, R.; Brody, A. S.; Light, M.; Skov, M.; Maish, W.; Mastella, G. Participants in the Cystic Fibrosis Foundation Consensus Conference. Allergic Bronchopulmonary Aspergillosis in Cystic Fibrosis—State of the Art:

Cystic Fibrosis Foundation Consensus Conference. *Clin. Infect. Dis.* **2003**, *37*, S225−S264.
(15) Pihet, M.; Carrere, J.; Cimon, B.; Chabasse, D.; Delhaes, L.; Symoens, F.; Bouchara, J. P. Occurrence and relevance of filamentous fungi in respiratory secretions of patients with cystic fibrosis–a review. *Med. Mycol.* **2009**, *47*, 387−397.
(16) Latgé, J. P. *Aspergillus fumigatus* and aspergillosis. *Clin. Microbiol. Rev.* **1999**, *12*, 310−350.
(17) Dagenais, T. R.; Keller, N. P. Pathogenesis of *Aspergillus fumigatus* in Invasive Aspergillosis. *Clin. Microbiol. Rev.* **2009**, *22*, 447−465.
(18) Margalit, A.; Kavanagh, K. The innate immune response to *Aspergillus fumigatus* at the alveolar surface. *FEMS Microbiol. Rev.* **2015**, *39*, 670−687.
(19) Daly, P.; Kavanagh, K. Pulmonary aspergillosis: clinical presentation; diagnosis and therapy. *Br. J. Biomed. Sci.* **2001**, *58*, 197−205.
(20) Agarwal, R. Allergic bronchopulmonary aspergillosis. *Chest* **2009**, *135*, 805−826.
(21) Kraemer, R.; Delosea, N.; Ballinari, P.; Gallati, S.; Crameri, R. Effect of allergic bronchopulmonary aspergillosis on lung function in children with cystic fibrosis. *Am. J. Respir. Crit. Care Med.* **2006**, *174*, 1211−1220.
(22) Kamath, K. S.; Kumar, S. S.; Kaur, J.; Venkatakrishnan, V.; Paulsen, I. T.; Nevalainen, H.; Molloy, M. P. Proteomics of hosts and pathogens in cystic fibrosis. *Proteomics: Clin. Appl.* **2015**, *9*, 134−146.
(23) Schlam, D.; Canton, J.; Carreno, M.; Kopinski, H.; Freeman, S. A.; Grinstein, S.; Fairn, G. D. Gliotoxin Suppresses Macrophage Immune Function by Subverting Phosphatidylinositol 3,4,5-Trisphosphate Homeostasis. *mBio* **2016**, *7*, No. e02242.
(24) Hector, A.; Kirn, T.; Ralhan, A.; Graepler-Mainka, U.; Berenbrinker, S.; Riethmueller, J.; Hogardt, M.; Wagner, M.; Pfleger, A.; Autenrieth, I.; Kappler, M.; Griese, M.; Eber, E.; Martus, P.; Hartl, D. Microbial colonization and lung function in adolescents with cystic fibrosis. *J. Cystic Fibrosis* **2016**, *15*, 340−349.
(25) Amin, R.; Dupuis, A.; Aaron, S. D.; Ratjen, F. The effect of chronic infection with *Aspergillus fumigatus* on lung function and hospitalization in patients with cystic fibrosis. *Chest* **2010**, *137*, 171−176.
(26) Leclair, L. W.; Hogan, D. A. Mixed bacterial-fungal infections in the CF respiratory tract. *Med Mycol.* **2010**, *48*, S125−S132.
(27) Smith, K.; Rajendran, R.; Kerr, S.; Lappin, D. F.; Mackay, W. G.; Williams, C.; Ramage, G. *Aspergillus fumigatus* enhances elastase production in *Pseudomonas aeruginosa* co-cultures. *Med. Mycol.* **2015**, *53*, 645−655.
(28) Chi, E.; Mehl, T.; Nunn, D.; Lory, S. Interaction of *Pseudomonas aeruginosa* with A549 pneumocyte cells. *Infect. Immun.* **1991**, *59*, 822−828.
(29) Daly, P.; Verhaegen, S.; Clynes, M.; Kavanagh, K. Culture filtrates of *Aspergillus fumigatus* induce different modes of cell death in human cancer cell lines. *Mycopathologia* **1999**, *146*, 67−74.
(30) Wasylnka, J. A.; Moore, M. M. Uptake of *Aspergillus fumigatus* Conidia by phagocytic and nonphagocytic cells in vitro: quantitation using strains expressing green fluorescent protein. *Infect. Immun.* **2002**, *70*, 3156−3163.
(31) Wasylnka, J. A.; Moore, M. M. *Aspergillus fumigatus* conidia survive and germinate in acidic organelles of A549 epithelial cells. *J. Cell Sci.* **2003**, *116*, 1579−1587.
(32) Zhang, Z.; Liu, R.; Noordhoek, J. A.; Kauffman, H. F. Interaction of airway epithelial cells (A549) with spores and mycelium of *Aspergillus fumigatus*. *J. Infect.* **2005**, *51*, 375−382.
(33) Hawdon, N. A.; Aval, P. S.; Barnes, R. J.; Gravelle, S. K.; Rosengren, J.; Khan, S.; Ciofu, O.; Johansen, H. K.; Hoiby, N.; Ulanova, M. Cellular responses of A549 alveolar epithelial cells to serially collected *Pseudomonas aeruginosa* from cystic fibrosis patients at different stages of pulmonary infection. *FEMS Immunol Med Microbiol.* **2010**, *59*, 207−220.
(34) Amin, S.; Thywissen, A.; Heinekamp, T.; Saluz, H. P.; Brakhage, A. A. Melanin dependent survival of *Apergillus fumigatus* conidia in lung epithelial cells. *Int. J. Med. Microbiol.* **2014**, *304*, 626−636.
(35) Hubner, N. C.; Bird, A. W.; Cox, J.; Splettstoesser, B.; Bandilla, P.; Poser, I.; Hyman, A.; Mann, M. Quantitative proteomics combined with BAC TransgeneOmics reveals in vivo protein interactions. *J. Cell Biol.* **2010**, *189*, 739−754.
(36) Jensen, L. J.; Kuhn, M.; Stark, M.; Chaffron, S.; Creevey, C.; Muller, J.; Doerks, T.; Julien, P.; Roth, A.; Simonovic, M.; Bork, P.; von Mering, C. STRING 8–a global view on proteins and their functional interactions in 630 organisms. *Nucleic Acids Res.* **2009**, *37*, D412−D416.
(37) Côté, R. G.; Griss, J.; Dianes, J. A.; Wang, R.; Wright, J. C.; van den Toorn, H. W. P.; van Breukelen, B.; Heck, A. J. R.; Hulstaert, N.; Martens, L.; Reisinger, F.; Csordas, A.; Ovelleiro, D.; Perez-Rivevol, Y.; Barsnes, H.; Hermjakob, H.; Vizcaíno, J. A. 2012. The PRoteomics IDEntification (PRIDE) Converter 2 framework: an improved suite of tools to facilitate data submission to the PRIDE database and the ProteomeXchange consortium. *Mol. Cell. Proteomics* **2012**, *11*, 1682−1689.
(38) Folkesson, A.; Jelsbak, L.; Yang, L.; Johansen, H. K.; Ciofu, O.; Hoiby, N.; Molin, S. Adaptation of *Pseudomonas aeruginosa* to the cystic fibrosis airway: an evolutionary perspective. *Nat. Rev. Microbiol.* **2012**, *10*, 841−851.
(39) Yang, L.; Jelsbak, L.; Molin, S. Microbial ecology and adaptation in cystic fibrosis airways. *Environ. Microbiol.* **2011**, *13*, 1682−1689.
(40) Salsgiver, E. L.; Fink, A. K.; Knapp, E. A.; LiPuma, J. J.; Olivier, K. N.; Marshall, B. C.; Saiman, L. Changing Epidemiology of the Respiratory Bacteriology of Patients With Cystic Fibrosis. *Chest* **2016**, *149*, 390−400.
(41) Sousa, A. M.; Pereira, M. O. *Pseudomonas aeruginosa* diversification during infection development in Cystic Fibrosis lungs − A Review. *Pathogens* **2014**, *3*, 680−703.
(42) Eisenreich, W.; Heesemann, J.; Rudel, T.; Goebel, W. Metabolic host responses to infection by intracellular bacterial pathogens. *Front. Cell. Infect. Microbiol.* **2013**, *3*, No. 24.
(43) Eisenreich, W.; Rudel, T.; Heesemann, J.; Goebel, W. To Eat and to Be Eaten: Mutual Metabolic Adaptations of Immune Cells and Intracellular Bacterial Pathogens upon Infection. *Front. Cell. Infect. Microbiol.* **2017**, *7*, No. 316.
(44) Ott, M.; Gogvadze, V.; Orrenius, S.; Zhivotovsky, B. Mitochondria; oxidative stress and cell death. *Apoptosis* **2007**, *12*, 913−922.
(45) Ivanov, A. V.; Bartosch, B.; Isaguliants, M. G. Oxidative Stress in Infection and Consequent Disease. *Oxid. Med. Cell. Longevity* **2017**, *2017*, No. 3496043.
(46) Mavrodi, D. V.; Bonsall, R. F.; Delaney, S. M.; Soule, M. J.; Phillips, G.; Thomashow, L. S. Functional analysis of genes for biosynthesis of pyocyanin and phenazine-1-carboxamide from *Pseudomonas aeruginosa* PAO1. *J. Bacteriol.* **2001**, *183*, 6454−6465.
(47) Liu, X.; Shao, K.; Sun, T. SIRT1 regulates the human alveolar epithelial A549 cell apoptosis induced by *Pseudomonas aeruginosa* lipopolysaccharide. *Cell. Physiol. Biochem.* **2013**, *31*, 92−101.
(48) Rada, B.; Leto, T. L. Pyocyanin effects on respiratory epithelium: relevance in *Pseudomonas aeruginosa* airway infections. *Trends Microbiol.* **2013**, *21*, 73−81.
(49) Hunter, R. C.; Klepac-Ceraj, V.; Lorenzi, M. M.; Grotzinger, H.; Martin, T. R.; Newman, D. K. Phenazine content in the cystic fibrosis respiratory tract negatively correlates with lung function and microbial complexity. *Am. J. Respir. Cell. Mol. Biol.* **2012**, *47*, 738−745.
(50) Galluzzi, L.; Kepp, O.; Kroemer, G. Mitochondria: master regulators of danger signalling. *Nat Rev. Mol. Cell. Biol.* **2012**, *13*, 780−788.
(51) Daly, P.; Kavanagh, K. Immobilization of *Aspergillus fumigatus* colonies in a soft agar matrix allows visualization of A549 cell detachment and death. *Med. Mycol.* **2002**, *40*, 27−33.
(52) Berkova, N.; Lair-Fulleringer, S.; Femenia, F.; Huet, D.; Wagner, M. C.; Gorna, K.; Tournier, F.; Ibrahim-Granet, O.; Guillot,

DOI: 10.1021/acs.jproteome.9b00520
J. Proteome Res. 2020, 19, 279−291

J.; Chermette, R.; Boireau, P.; Latge, J. P. *Aspergillus fumigatus* conidia inhibit tumour necrosis factor- or staurosporine-induced apoptosis in epithelial cells. *Int. Immunol.* **2006**, *18*, 139−150.
(53) Heinekamp, T.; Schmidt, H.; Lapp, K.; Pahtz, V.; Shopova, I.; Koster-Eiserfunke, N.; Kruger, T.; Kniemeyer, O.; Brakhage, A. A. Interference of *Aspergillus fumigatus* with the immune response. *Semin. Immunopathol.* **2015**, *37*, 141−152.
(54) Fontana, M. F.; Banga, S.; Barry, K. C.; Shen, X.; Tan, Y.; Luo, Z. Q.; Vance, R. E. Secreted bacterial effectors that inhibit host protein synthesis are critical for induction of the innate immune response to virulent *Legionella pneumophila*. *PLoS Pathog.* **2011**, *7*, No. e1001289.
(55) Fontana, M. F.; Shin, S.; Vance, R. E. Activation of host mitogen-activated protein kinases by secreted *Legionella pneumophila* effectors that inhibit host protein translation. *Infect. Immun.* **2012**, *80*, 3570−3575.
(56) Dunbar, T. L.; Yan, Z.; Balla, K. M.; Smelkinson, M. G.; Troemel, E. R. *C. elegans* detects pathogen-induced translational inhibition to activate immune signaling. *Cell Host Microbe* **2012**, *11*, 375−386.
(57) Mohr, I.; Sonenberg, N. Host translation at the nexus of infection and immunity. *Cell Host Microbe* **2012**, *12*, 470−483.
(58) McEwan, D. L.; Kirienko, N. V.; Ausubel, F. M. Host translational inhibition by *Pseudomonas aeruginosa* Exotoxin A Triggers an immune response in *Caenorhabditis elegans*. *Cell Host Microbe* **2012**, *11*, 364−374.
(59) van 't Wout, E. F.; van Schadewijk, A.; van Boxtel, R.; Dalton, L. E.; Clarke, H. J.; Tommassen, J.; Marciniak, S. J.; Hiemstra, P. S. Virulence Factors of *Pseudomonas aeruginosa* Induce Both the Unfolded Protein and Integrated Stress Responses in Airway Epithelial Cells. *PLoS Pathog.* **2015**, *11*, No. e1004946.
(60) Celli, J.; Tsolis, R. M. Bacteria; the endoplasmic reticulum and the unfolded protein response: friends or foes? *Nat. Rev. Microbiol.* **2015**, *13*, 71−82.
(61) Jeong, J. S.; Kim, S. R.; Lee, Y. C. Can Controlling Endoplasmic Reticulum Dysfunction Treat Allergic Inflammation in Severe Asthma With Fungal Sensitization? *Allergy Asthma Immunol. Res.* **2018**, *10*, 106−120.
(62) Lee, K. S.; Jeong, J. S.; Kim, S. R.; Cho, S. H.; Kolliputi, N.; Ko, Y. H.; Lee, K. B.; Park, S. C.; Park, H. J.; Lee, Y. C. Phosphoinositide 3-kinase-delta regulates fungus-induced allergic lung inflammation through endoplasmic reticulum stress. *Thorax* **2016**, *71*, 52−63.
(63) Kim, S.; Joe, Y.; Park, S. U.; Jeong, S. O.; Kim, J. K.; Park, S. H.; Pae, H. O.; Surh, Y. J.; Shin, J.; Chung, H. T. Induction of endoplasmic reticulum stress under endotoxin tolerance increases inflammatory responses and decreases *Pseudomonas aeruginosa* pneumonia. *J. Leukoc. Biol.* **2018**, *104*, 1003−1012.
(64) Jiang, F.; Wang, X.; Wang, B.; Chen, L.; Zhao, Z.; Waterfield, N. R.; Yang, G.; Jin, Q. The *Pseudomonas aeruginosa* Type VI Secretion PGAP1-like Effector Induces Host Autophagy by Activating Endoplasmic Reticulum Stress. *Cell Rep.* **2016**, *16*, 1502−1509.
(65) Gurbuxani, S.; Schmitt, E.; Cande, C.; Parcellier, A.; Hammann, A.; Daugas, E.; Kouranti, I.; Spahr, C.; Pance, A.; Kroemer, G.; Garrido, C. Heat shock protein 70 binding inhibits the nuclear import of apoptosis-inducing factor. *Oncogene* **2003**, *22*, 6669−6678.
(66) Frese, S.; Schaper, M.; Kuster, J.-R.; Miescher, D.; Jäättelä, M.; Buehler, T.; Schmid, R. A. Cell death induced by down-regulation of heat shock protein 70 in lung cancer cell lines is p53-independent and does not require DNA cleavage. *J. Thorac. Cardiovasc. Surg.* **2003**, *126*, 748−754.
(67) Liu, W.; Chen, Y.; Lu, G.; Sun, L.; Si, J. Down-regulation of HSP70 sensitizes gastric epithelial cells to apoptosis and growth retardation triggered by *H. pylori*. *BMC Gastroenterol.* **2011**, *11*, No. 146.
(68) Sharon, H.; Amar, D.; Levdansky, E.; Mircus, G.; Shadkchan, Y.; Shamir, R.; Osherov, N. PrtT-regulated proteins secreted *Aspergillus fumigatus* activate MAPK signaling in exposed A549 lung cells leading to necrotic cell death. *PLoS One* **2011**, *6*, No. e17509.
(69) Balloy, V.; Sallenave, J. M.; Wu, Y.; Touqui, L.; Latge, J. P.; Si-Tahar, M.; Chignard, M. *Aspergillus fumigatus*-induced interleukin-8 synthesis by respiratory epithelial cells is controlled by the phosphatidylinositol 3-kinase; p38 MAPK; and ERK1/2 pathways and not by the toll-like receptor-MyD88 pathway. *J. Biol. Chem.* **2008**, *283*, 30513−30521.
(70) So, J. S. Roles of Endoplasmic Reticulum Stress in Immune Responses. *Mol. Cells* **2018**, *41*, 705−716.
(71) Li, J.; Chai, Q. Y.; Liu, C. H. The ubiquitin system: a critical regulator of innate immunity and pathogen-host interactions. *Cell. Mol. Immunol.* **2016**, *13*, 560−576.
(72) Lapaquette, P.; Guzzo, J.; Bretillon, L.; Bringer, M. A. Cellular and Molecular Connections between Autophagy and Inflammation. *Mediators Inflammation* **2015**, *2015*, No. 398483.
(73) Maculins, T.; Fiskin, E.; Bhogaraju, S.; Dikic, I. Bacteria-host relationship: ubiquitin ligases as weapons of invasion. *Cell Res.* **2016**, *26*, 499−510.
(74) Bomberger, J. M.; Ely, K. H.; Bangia, N.; Ye, S.; Green, K. A.; Green, W. R.; Enelow, R. I.; Stanton, B. A. *Pseudomonas aeruginosa* Cif protein enhances the ubiquitination and proteasomal degradation of the transporter associated with antigen processing (TAP) and reduces major histocompatibility complex (MHC) class I antigen presentation. *J. Biol. Chem.* **2014**, *289*, 152−162.
(75) Bomberger, J. M.; Ye, S.; Maceachran, D. P.; Koeppen, K.; Barnaby, R. L.; O'Toole, G. A.; Stanton, B. A. A *Pseudomonas aeruginosa* toxin that hijacks the host ubiquitin proteolytic system. *PLoS Pathog.* **2011**, *7*, No. e1001325.
(76) Malet, J. K.; Impens, F.; Carvalho, F.; Hamon, M. A.; Cossart, P.; Ribet, D. Rapid Remodeling of the Host Epithelial Cell Proteome by the Listeriolysin O (LLO) Pore-forming Toxin. *Mol. Cell. Proteomics* **2018**, *17*, 1627−1636.
(77) Vos, J. B.; van Sterkenburg, M. A.; Rabe, K. F.; Schalkwijk, J.; Hiemstra, P. S.; Datson, N. A. Transcriptional response of bronchial epithelial cells to *Pseudomonas aeruginosa*: identification of early mediators of host defense. *Physiol. Genomics* **2005**, *21*, 324−336.
(78) Lavoie, E. G.; Wangdi, T.; Kazmierczak, B. I. Innate immune responses to *Pseudomonas aeruginosa* infection. *Microbes Infect.* **2011**, *13*, 1133−1145.
(79) Zhou, H.; Monack, D. M.; Kayagaki, N.; Wertz, I.; Yin, J.; Wolf, B.; Dixit, V. M. Yersinia virulence factor YopJ acts as a deubiquitinase to inhibit NF-kappa B activation. *J. Exp. Med.* **2005**, *202*, 1327−1332.
(80) Ashida, H.; Kim, M.; Schmidt-Supprian, M.; Ma, A.; Ogawa, M.; Sasakawa, C. A bacterial E3 ubiquitin ligase IpaH9.8 targets NEMO/IKKgamma to dampen the host NF-kappaB-mediated inflammatory response. *Nat. Cell Biol.* **2010**, *12*, 66−73.
(81) Zhao, K.; Li, W.; Li, J.; Ma, T.; Wang, K.; Yuan, Y.; Li, J. S.; Xie, R.; Huang, T.; Zhang, Y.; Zhou, Y.; Huang, N.; Wu, W.; Wang, Z.; Zhang, J.; Yue, B.; Zhou, Z.; Li, J.; Wei, Y. Q.; Zhang, X.; Zhou, X. TesG is a type I secretion effector of *Pseudomonas aeruginosa* that suppresses the host immune response during chronic infection. *Nat. Microbiol.* **2019**, *4*, 459−469.
(82) May, R. C.; Machesky, L. M. Phagocytosis and the actin cytoskeleton. *J. Cell Sci.* **2001**, *114*, 1061−1077.
(83) Sana, T. G.; Baumann, C.; Merdes, A.; Soscia, C.; Rattei, T.; Hachani, A.; Jones, C.; Bennett, K. L.; Filloux, A.; Superti-Furga, G.; Voulhoux, R.; Bleves, S. Internalization of *Pseudomonas aeruginosa* Strain PAO1 into Epithelial Cells Is Promoted by Interaction of a T6SS Effector with the Microtubule Network. *mBio* **2015**, *6*, No. e00712.
(84) Akoumianaki, T.; Kyrmizi, I.; Valsecchi, I.; Gresnigt, M. S.; Samonis, G.; Drakos, E.; Boumpas, D.; Muszkieta, L.; Prevost, M. C.; Kontoyiannis, D. P.; Chavakis, T.; Netea, M. G.; van de Veerdonk, F. L.; Brakhage, A. A.; El-Benna, J.; Beauvais, A.; Latge, J. P.; Chamilos, G. Aspergillus Cell Wall Melanin Blocks LC3-Associated Phagocytosis to Promote Pathogenicity. *Cell Host Microbe* **2016**, *19*, 79−90.
(85) Bertout, S.; Badoc, C.; Mallie, M.; Giaimis, J.; Bastide, J. M. Spore diffusate isolated from some strains of *Aspergillus fumigatus* inhibits phagocytosis by murine alveolar macrophages. *FEMS Immunol. Med. Microbiol.* **2002**, *33*, 101−106.

DOI: 10.1021/acs.jproteome.9b00520
J. Proteome Res. 2020, 19, 279−291

(86) Deng, Q.; Barbieri, J. T. Molecular mechanisms of the cytotoxicity of ADP-ribosylating toxins. *Annu. Rev. Microbiol.* **2008**, *62*, 271−288.
(87) Krall, R.; Schmidt, G.; Aktories, K.; Barbieri, J. T. *Pseudomonas aeruginosa* ExoT is a Rho GTPase-activating protein. *Infect. Immun.* **2000**, *68*, 6066−6068.
(88) Popoff, M. R. Bacterial factors exploit eukaryotic Rho GTPase signaling cascades to promote invasion and proliferation within their host. *Small GTPases* **2014**, *5*, No. e28209.
(89) Uribe-Querol, E.; Rosales, C. Control of Phagocytosis by Microbial Pathogens. *Front. Immunol.* **2017**, *8*, No. 1368.
(90) Angus, A. A.; Lee, A. A.; Augustin, D. K.; Lee, E. J.; Evans, D. J.; Fleiszig, S. M. *Pseudomonas aeruginosa* induces membrane blebs in epithelial cells; which are utilized as a niche for intracellular replication and motility. *Infect. Immun.* **2008**, *76*, 1992−2001.
(91) Wasylnka, J. A.; Hissen, A. H.; Wan, A. N.; Moore, M. M. Intracellular and extracellular growth of *Aspergillus fumigatus*. *Med. Mycol.* **2005**, *43*, S27−S30.

DOI: 10.1021/acs.jproteome.9b00520
J. Proteome Res. 2020, 19, 279−291